

Multi-contour registration based on feature points correspondence and two-stage gene expression programming



Xiuyang Zhao ^a, Bo Yang ^{a,*}, Shuming Gao ^b, Yuehui Chen ^a

^a Shandong Provincial Key Laboratory of Network based Intelligent Computing, University of Jinan, Jinan 250022, China

^b State Key Laboratory of CAD&CG, Zhejiang University, Hangzhou 310058, China

ARTICLE INFO

Article history:

Received 18 September 2012

Received in revised form

15 April 2014

Accepted 5 May 2014

Communicated by A. Abraham

Available online 15 May 2014

Keywords:

Contour registration

Foot point

GEP

Feature point

CPSO

B-spline

ABSTRACT

Image registration is a fundamental task in 3D reconstruction from an image sequence. Although this topic has been studied for decades, a general, robust, and automatic image registration method is rare, and most existing image registration methods are designed for a particular application. In this paper, image registration is treated as a formula discovery problem. A novel contour registration pipeline was proposed based on a foot-point-based feature point correspondence algorithm and a two-stage evolutionary algorithm. Our proposal has three objectives. First, we introduce a novel feature point extraction method that uses estimation of the curvature and the support region for every contour in the floating image. Second, we approximate the reference contour using a Gaussian mixture model (GMM) continuous optimization algorithm followed by an order-preserved foot-point detection method used to extract the feature points that correspond to the feature points of the floating contours. Third, we propose a hybrid evolutionary algorithm used to identify the registration formula for the reference image and the floating image. The hybrid evolutionary algorithm is a two-stage algorithm based on gene expression programming (GEP) and the improved cooperative particle swarm optimizer (CPSO). The optimal or near-optimal structure is accomplished using the GEP algorithm, and the parameters embedded in the structure are optimized by an opposition based learning (OBL)-based cooperative particle swarm optimizer (CPSO). Compared with other non-rigid registration methods, the developed registration pipeline produces competitive results with high accuracy.

© 2014 Published by Elsevier B.V.

1. Introduction

Image registration is a fundamental task in 3D reconstruction that addresses the geometric alignment of a set of images. The set may consist of two or more digital images taken of a single scene at different times, from different sensors, or from different viewpoints [1]. Many methods have been proposed to address this problem. A popular approach involves treating the salient features of the image as invariant to find the geometric transformation [2]. Using a feature-based method, a number of relevant image features are first extracted from the two images, the correspondences between the feature points are subsequently identified, and a geometric matching transformation is used to provide the best match for the two sets of features.

The most common methods of feature extraction are the contour-based hierarchical method [3] and the scale invariant feature transform [4]. The general feature correspondence algorithms include the assignment algorithm [5], the graph-matching

method [6], the speeded-up robust features approach [7], and the expectation conditional maximization algorithms [8]. The transformation parameters estimation method is carried out based on the detection of features that have undergone feature correspondence. In most existing feature-based techniques, the feature correspondence is still the most challenging problem.

The feature-points-based contour matching problem can be carried out as follows [9]: first, we extract a set of feature points from each object, e.g., by running an edge detector over each image and sampling from the edges. Second, we determine the pairs of corresponding features in the two feature sets. Third, we use the correspondence information to find an aligning transformation, such as the least squares transformation from a certain class.

An interesting subject in contour matching is a contour simplification that preserves the original characteristics of shape features. The feature points are those points that exhibit extreme values on the curve and that can suitably describe the curve for visual perception and recognition. The most obvious advantage of using feature points to represent the contours is the large effect on data reduction and its immediate impact on the efficiency of the subsequent contour-matching algorithms. As described in

* Corresponding author.

E-mail address: yangbo@ujn.edu.cn (B. Yang).

references [10–11], there are three major categories of methods used to detect the feature points:

- (1) Methods that search for feature points from the original contour scale or from a multi-scale contour representation using a significant measure other than curvature.
- (2) Methods that evaluate the curvature by transforming the contour to the Gaussian scale space.
- (3) Methods that search for feature points by directly estimating the curvature in the original picture space.

In this paper, an improved contour simplification method that uses a polygonal approximation is proposed. The new strategy is based on the method proposed by Wu [12–13], which determines the region of support in finding the feature points.

The second stage of determining the point correspondences has been the subject of much research. Intuitively, one would expect an exact one-to-one correspondence between the reference contour and the floating contour. An increasingly popular approach involves building a cost matrix that records the dissimilarity between all possible pairs of points on the two shapes. The unconstrained optimal assignment problem is essentially determined by the cost matrix. If we can guarantee that all entries in the cost matrix are integral or rational numbers, the Hungarian algorithm is a good choice for arriving at one optimal solution with a finite number of iterations. Another category of solutions to the correspondence problem alternates the estimations of correspondence and transformation. The iterative closest point (ICP) algorithm [14] is the best known and most widely used among these methods, it uses the nearest-neighbor relationship to assign a binary correspondence at each step. Reference [15] enhanced this algorithm with two significant improvements: the soft-assign idea and the Robust Point Matching-Thin Plate Spline (RPMTPS) algorithm. Li et al. [16] presented an automatic approach based on multidimensional scaling to match the correspondences on 3-D human bodies in various postures, but their aim was to extract the feature points automatically. In reference [17], the problem of automatic determination of the point correspondence between two images was formulated as a multimodal function optimization, and genetic algorithms (GAs) were used to solve the optimization problem. Reference [18] proposed a method for non-rigid point-matching based on a shape context descriptor. The shape context describes the coarse distribution of the remainder of the shape with respect to a given point on the shape, parameterized by distance and angular extent with respect to the point described. The solution that minimizes the overall shape context distances becomes the optimal match between the two point sets. Although this approach has produced encouraging results in various application fields [19–20], the neighboring points in one shape may be matched to two points that are far apart in the other shape because the method is defective in its spatial ordering constraints.

The third stage for finding aligning transformations can be treated as a problem of formula discovery [38]. Formula discovery aims to identify a formula that describes the relationship between the independent variable and dependent variable using a large number of test data. The common mathematical methods for resolving formula discovery are the curve-fitting method, the regression analysis method, approximation theory and genetic programming algorithms, among others. Genetic programming (GP) algorithms have certain advantages compared with other methods. In addition to the obvious benefit of automation, the GP provides power and flexibility that potentially allow for formula evolution.

Gene expression programming (GEP), as an extension of GP, is an evolutionary algorithm that automatically creates complex tree structures that learn and adapt by changing their sizes, shapes, and composition [21]. As the natural development of GA and GP,

GEP combines the genotype of GA and the phenotype of GP. The genome of GEP consists of a linear, symbolic string or chromosome of fixed length composed of one or more genes of equal size. The chromosome can be evolved by mutation, recombination, transposition and so on [25]. All the genes of gene expression programming have the same size. However, these fixed length strings code for expression trees of different sizes. This means that the size of the coding regions varies from gene to gene, allowing for adaptation and evolution to occur smoothly. GEP overcomes many limitations of GA and GP, so it has been widely used in problem solving such as regression, classification, cluster etc.

In this study, we introduce a new model to address the formula discovery problem. Different from [24], the proposed model is a two-stage evolutionary algorithm based on GEP and an improved cooperative particle swarm optimizer. The optimal or near-optimal structure is found using the GEP algorithm, and the parameters embedded in the structure are optimized by an opposition-based-learning (OBL)-based cooperative particle swarm optimizer (CPSO). We refer to the two-stage evolutionary algorithm as CGEPSOBL. The two-stage evolutionary algorithm contains certain similarities to the flexible neural tree (FNT) algorithm, but the most distinctive feature of our algorithm is that CGEPSOBL can generate multi-expressions rather than a single expression.

This paper proposes a novel contour registration pipeline based on a foot-point-based feature point correspondence algorithm and a new evolutionary algorithm known as CGEPSOBL. At the feature point detection stage, we propose a novel feature point extraction method based on the signed discrete curvature calculation and the adaptive bending value estimation. At the stage of determining the pairs of feature points, we propose an integrated method that combines the feature point detection and pairs of features point determination. At the stage of finding the alignment transformation, the new model known as CGEPSOBL is used to identify the registration formula of the reference image and the floating image.

This paper contains two major contributions. First, we introduce an integrated method that detects the feature points of the reference image and matches the point sets simultaneously. Our approach is based on three-order B-spline approximation and foot-point detection. The classical methods commonly extract the feature points first and find the match afterwards. The drawback of the classical method is that the feature point detection and the matching are separated. An advantage of our method is that the feature point detection and the matching are integrated, and the method is sufficiently able to mine the information of the reference contours described by the B-spline curves and find the most appropriate feature points on the reference contours. Second, we propose a two-stage hybrid evolutionary algorithm, GEP is used to construct the basic structure because it can automatically establish a relational model between the given input variables and output variables. The parameters embedded in the basic structure are optimized by the OBL-based CPSO (CPSOBL) algorithm. Compared with the standard PSO, the CPSOBL algorithm contains higher diversity. The higher diversity ensures that the search space is searched more thoroughly and that the algorithm has a greater chance of reaching the global solution.

The remainder of the paper is organized as follows. The feature point detection and correspondence methods are described in Section 2. Section 3 presents the details of the proposed two-stage hybrid evolutionary algorithm. In Section 4, the results of experiments are discussed and compared with those of other methods. Section 5 concludes the paper.

2. Feature points detection and correspondence

The correspondence problem is usually based on two sets of feature points. The correspondence result of this type of method

depends heavily on the inherit similarity of the two point sets. In this paper, a new algorithm is proposed to address the correspondence problem. The algorithm includes three steps. First, for every contour in the floating image, calculate its similarity to every contour in the reference image. Based on the cost matrix constituted by the similarities, we can get the one to one correspondence of the contours from different images, i.e. contour pairs. Second, for every contour pairs, the floating contour is sampled with the algorithm described in Section 2.2 and the reference contour is approximated by the B-spline curve. Third, for every contour pairs, the feature points in the floating contour are mapping to the B-spline curve of the reference contour. The foot point on the B-spline curve is the sample data of the reference contour. Thus we can acquire the feature points on the reference contour and the feature point pairs simultaneously.

2.1. Contours correspondence

Two representative and successive cement images are shown in Fig. 1. The successive images contain a varying number of cement particles. Therefore, we must determine the correspondence of the contours.

In this paper, we define the corresponding contour pairs using the comparability and the location of the contours in the floating image and the reference image. The comparability is calculated by

$$R = \frac{\sum_{i=1}^7 \phi_i^s \phi_i^x}{\left(\sum_{i=1}^7 (\phi_i^s)^2 \sum_{j=1}^7 (\phi_j^x)^2 \right)^{1/2}}, \quad (1)$$

where $\phi_i^s(k) (k=1, \dots, 7)$ is the i th contour's invariant moments of the floating image, and $\phi_i^x(k) (k=1, \dots, 7)$ is the j th contour's invariant moments of the reference image.

The correspondence is an assignment problem, and the cost matrix is constructed using the similarity of contours. Based on the solution of the cost matrix by the Hungarian method, we can acquire the one to one correspondence of the contours from different images.

2.2. Feature points detection

The contours obtained by the edge detection algorithm are always discrete and out of order. In this section, we attempt to represent a contour with a limited number of feature points located along the contours. The points with high curvature contain significant information that can describe the contour, but these points are usually unevenly located along the contour and are sensitive to noise. Therefore, a curvature-estimation-based method is given to find the feature points. The feature point detection

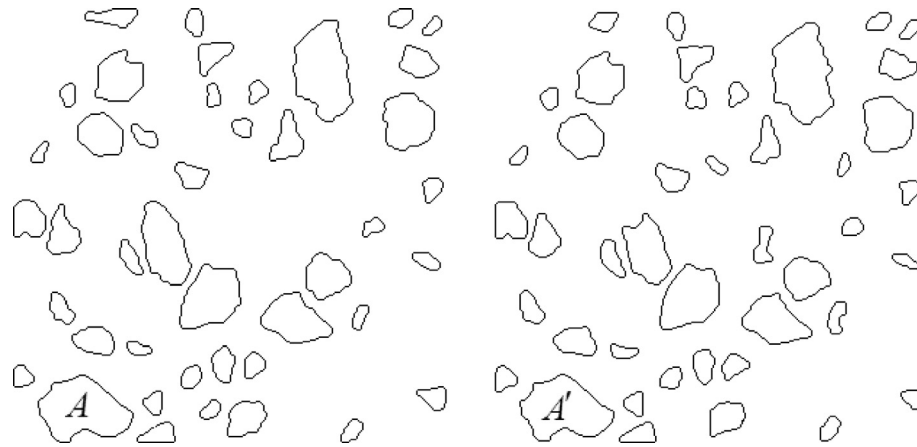


Fig. 1. The successive images of cement [42].

includes three steps: selection of the points with high curvature as candidate points, curvature estimation and identification of the feature points.

In a Euclidean space, the curvature is defined as the instantaneous rate of the slope change and is a function of the arc length at a corresponding point. For an ordered point set $S = \{s_i(x_i, y_i) | i = 0, 1, \dots, n\}$, the discrete curvature k_i at point $s_i (i = 1, \dots, n-1)$ is defined as the inverse of the radius r_i of the circle passing through the three points s_{i-1}, s_i and s_{i+1} , as illustrated in Fig. 2.

The signed discrete curvature can be expressed as [22–23]

$$k_i = \frac{2\Delta s_{i-1}s_i s_{i+1}}{L_i L_{i+1} Q_i} = \text{sign}(\Delta s_{i-1}s_i s_{i+1}) \frac{2 \sin(\alpha_i)}{Q_i}, \quad (2)$$

where

$$Q_i = s_{i+1} - s_{i-1}, \quad Q_i = \|Q_i\|, \quad L_i = p_i - p_{i-1}, \quad L_i = \|L_i\|,$$

$$\Delta s_{i-1}s_i s_{i+1} = \det(L_i, L_{i+1}), \quad \cos(\alpha_i) = \frac{L_i L_{i+1}}{|L_i L_{i+1}|}.$$

Those points whose curvature is greater than a threshold η can be treated as candidate points. The curvature calculated in Eq. (1) is illustrated by Figs. 3 and 4.

The adaptive bending value is used to determine the support region for each candidate point on the curve. The bending value is defined as [12]

$$b_{ik} = \max(|(x_{i-k} - x_i) + (x_{i+k} - x_i)|, |(y_{i-k} - y_i) + (y_{i+k} - y_i)|), \quad (3)$$

The length of the support regions can be determined by finding the inflection point around every candidate point. Once the support region for each candidate point is determined, the estimated curvature can be obtained by the following equation [12–13]:

$$bv_i = \frac{1}{k_i} \sum_{j=1}^{k_i} b_{ij}, \quad (4)$$

Based on the estimated curvature of every candidate point, the feature points are identified by three conditions given as follows.

a) If $bv_i < \epsilon$, the dominant point must be deleted, and ϵ is a pre-set threshold;

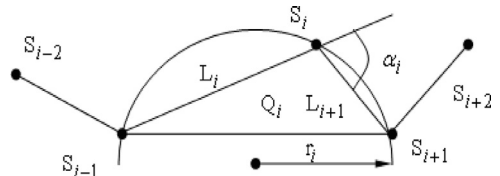


Fig. 2. Discrete curvature of ordered points.

- b) If two neighboring feature points exist, the dominant point with the smaller estimated curvature must be deleted; if the two neighboring feature points have equal estimated curvatures, the one with the smaller support region must be deleted;
c) The remaining points are the feature points.

2.3. Foot-point-based feature point correspondence

The aim in point matching is to find one-to-one correspondences between two given datasets [28]. Finding the correspondences between feature points belonging to non-rigid objects are not only a more challenging but also a potentially more important task. For 2D shapes, the correspondence between the boundary curves of the individual shapes is often defined by manual land marking [7]. Although this approach is feasible, it is a rather time-consuming and error-prone task [29]. In the automatic point correspondence approaches [16,30], the correspondence and the transformation are determined iteratively. Once the correspondence of the feature points is given, the transformation can be determined with reasonable knowledge. However, the correspondence can be searched if the transformation is known. Hence, this process leads to a solution of the correspondence problem by alternating the estimations of correspondence and transformation.



Fig. 3. Two composite contours.

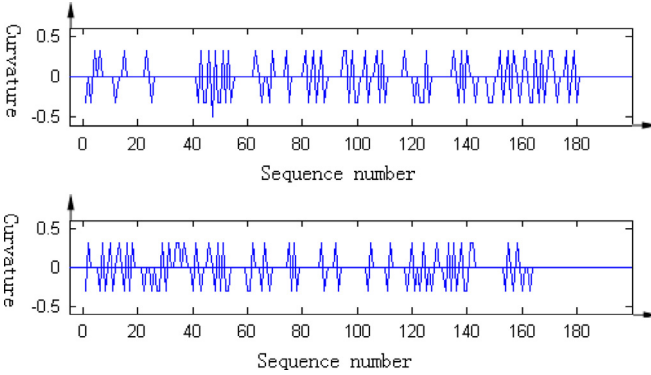


Fig. 4. Discrete curvature of the two contours.

In this paper, we first extracted the feature points of the floating contour using the curvature estimation method described in [Section 2](#), and subsequently approximated the reference contour via a Gaussian mixture model (GMM) continuous optimization algorithm [40] to acquire the B-spline curves. The feature points on the floating contour are mapped to the corresponding reference contour described by the B-spline curve, and the order-preserved foot points on the B-spline curve can be viewed as the feature points of the reference contour. Therefore, we complete the feature point extraction and solve the correspondence problem simultaneously.

Let $X_k \in R^2, k = 1, 2, \dots, n$ be organized data points representing a floating contour in the floating image and the corresponding reference contour is described by a closed planar B-spline curve $P(t)$. The closest point of X_k on $P(t)$ can be acquired by minimizing $g(t) = \|P(t) - X_k\|^2$, [\(5\)](#)

For a minimizer t_k of $g(t)$, $P(t_k)$ is called the foot point of X_k on $P(t)$. The equation can be minimized using Newton iteration.

Because the feature points of every contour in the floating image are ordered data points and the B-spline curve is a parameterized curve, we can easily preserve the foot-point order using the method described in the literature [32].

Based on the feature points in the floating image extracted in [Section 2.2](#), we calculate the foot points on the corresponding reference contours. For example, as shown in [Fig. 1](#), contours A and A' are corresponding contour pairs in the floating and the reference image, respectively. The feature points of A and the B-spline approximation curve of A' are shown in [Fig. 5a](#). The feature points of the reference contour and the corresponding are shown in [Fig. 5b](#). If the B-spline curve is complicated, we will evolve it toward the feature points of the floating contour by using the SDM method, and then the correspondence of feature points will be acquired by backtracking with the same parameter in the B-spline curve.

3. Formula discovery based on a two-stage hybrid evolutionary algorithm

In this study, we propose a new evolutionary model to address the formula discovery problem. The evolutionary model first evolves an optimal or near-optimal basic expression using the GEP algorithm and subsequently finds the optimal parameter set of the basic structure using the OBL-based CPSO.

The two stages of the model have an inherited relationship, and a balance exists between the basic structure optimization and the parameter learning [26–27]. The basic structure of the evolved model is the foundation, and therefore, an optimal or near-optimal basic structure is needed; otherwise, further basic structure optimization is

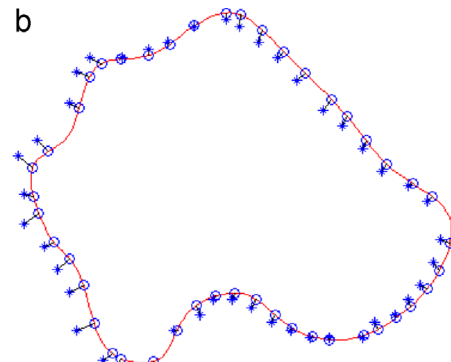


Fig. 5. Foot-point-based feature point matching example.

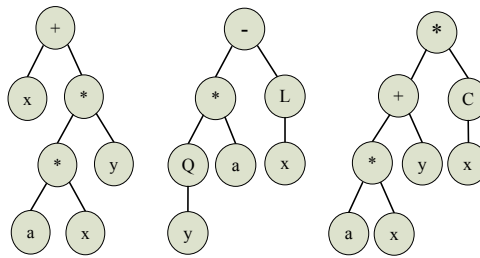


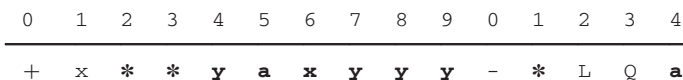
Fig. 6. An example of a chromosome.

nonsensical. However, an optimal or near optimal basic structure is still far from sufficient, and thus, further optimization of the basic structure may yield a better experiment result. In addition, we should pay attention to the damage to the basic structure during the stage of parameter optimization. In this paper, we achieve the balance using a trial-and-error method. If a better structure is found, then the parameter optimization searches for a number of steps or stops in the case in which no better parameter vector is found over a significantly long time (e.g., 200–1000 iterations in our experiments). The criterion for a better structure is distinguished as follows: if the fitness value of the best program is smaller than the fitness value of the elitist program or the fitness values of two programs are equal but the length of the former substring is lower than the latter ones, then we conclude that a better structure is found.

3.1. Basic structure optimization using GEP

In this section, an optimized expression is acquired to find the registration formula using GEP. In this method, the genome or chromosome consists of a linear, symbolic string of fixed length composed of one or more genes. GEP genes are composed of a head and a tail. The length of the head h and the length of the tail t have clear relationship $t=h(n-1)+1$, where n is the largest arity of the functions used in the gene's head. Despite its fixed length, each gene can code expression trees (ETs) with different sizes and shapes. GEP chromosomes are usually composed of more than one gene of equal length and each gene codes for a sub-ET. The sub-ETs may form a more complex multi-subunit ET by one or several linking function. In this paper, the fitness of sub-ETs and the multi-subunit ET is computed, and the best one is chosen to represent the chromosome.

An example of a chromosome with length 27, composed of three genes, is shown in Fig. 6, with the corresponding ETs, where Q , C and L are square root function, cosines and logarithm respectively. In the example, $h=4$ and $t=5$, the length of each gene is $4+5=9$. The tail is shown in bold.



The sub-expression trees can interact with each other and generate complete expression with the help of linking functions. The linking functions can be “+, −, *, /”, and so on. If we link the genes in Fig. 6 using subtraction and addition, the final ET could be linearly encoded as the following K-expression:

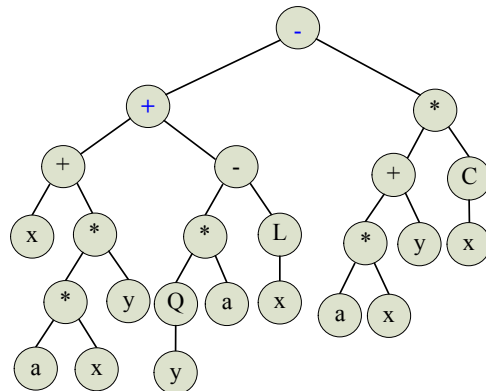
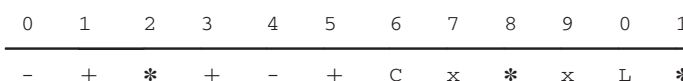


Fig. 7. An example of a chromosome with linking functions. (For interpretation of the references to color in this figure, the reader is referred to the web version of this article)

Fig. 7 shows final ET, and the symbols in blue are the linking functions.

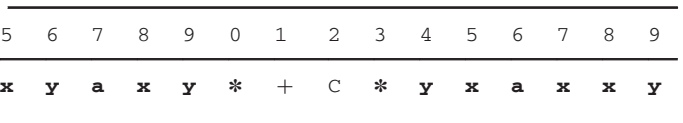
In our method, the terminal set T is $\{a, x_1, x_2\}$ (where a is a real number), and the function set F is $\{+, -, \times, \div, \text{square}, \cos, \sin, \log, \sqrt{\cdot}\}$. The genetic operators for the GEP algorithm used in this paper are crossover and mutation. Application of these operators preserves the chromosome structure, and all offspring represent syntactically correct expressions.

In this paper, the fitness function is based on overlap rate of the polygon enclosed by the feature points. The overlap rate evaluation is performed using Dice ratio defined as

$$D(U, V) = 2 \times |U \cap V| / (|U| + |V|), \quad (6)$$

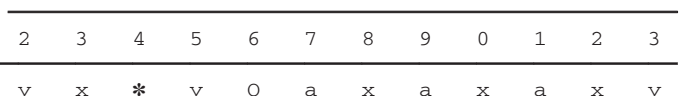
where U and V are two regions of the corresponding polygon in the two different images, and $| \cdot |$ denotes the area of a region [31]. The reason of using the overlap rate as fitness function is twofold: first, we would like to match as much feature points as possible, the overlap rate would decrease if there are a lot of feature points mismatched; second, we would like the feature points matched in a cyclic order preserving manner, an intersecting match will decrease the overlap rate too.

At the beginning of the optimization process, individuals are generated via random fabrication using the terminal set and the function set. The population is created with a randomly selected set of individuals. We compute the fitness of each sub-expression encoded in the GEP chromosome, and the fitness of the entire individual is measured by the fitness of the best expression encoded in that chromosome. After many generations of genetic operations, the best expression in the population is selected as the optimizing expression.



3.2. Parameter optimization using CPSOBL

Evolutionary algorithms constitute a universal optimization method that imitates the genetic adaptation occurring in natural evolution [33]. Unlike specialized methods designed for particular types of optimization tasks, these algorithms require no particular



knowledge of the problem structure other than the objective function itself. A population of candidate solutions evolve over time by means of genetic operators such as mutation, recombination and selection. For searching the coefficients in the given expression, an improved PSO is chosen to find the global optimal coefficients for the registration formula.

3.2.1. PSO algorithm

The PSO is a stochastic population-based optimization method that has been applied successfully to a wide range of problems [34]. In the PSO algorithm, a swarm of individuals (referred to as particles) fly through the search space. Each particle represents a candidate solution to the optimization problem. Each solution to a certain problem is

represented by a particle in the search space. All of these particles form a population. The flight direction and the distance traveled for each particle are both decided by its velocity. Next, each of the particles flies through the solution space following its best position visited (i.e., its own experience) and the position of the best particle in its neighborhood (i.e., the experience of the neighboring particles). After a certain number of iterations, the position vector of the best particle will represent an approximate optimum solution to the problem.

The PSO algorithm first initializes the population with a group of random particles and iteratively searches for the optimum solution. The particles update themselves by tracking two vectors: the best solution found by the particle itself *pbest* and the best solution found by the population *gbest*. In each step of the

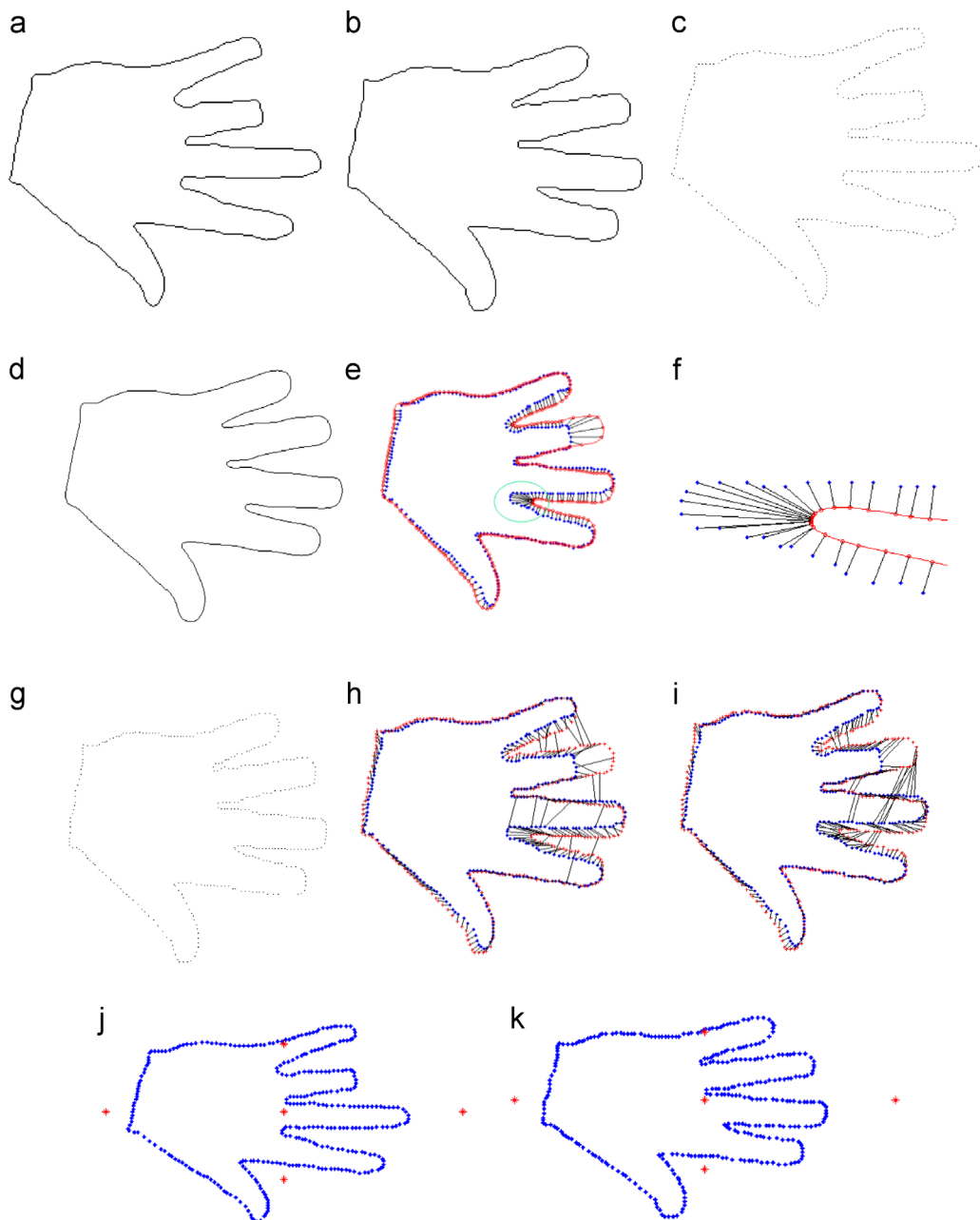


Fig. 8. Hand data sets, feature point samples and assignment: (a) floating image, (b) reference image, (c) feature points of the floating image, (d) B-spline contour of the reference image, (e) feature points detection on the B-spline contour of the reference image, (f) highlights of the marked part with magnified views, (g) feature points of the reference image, (h) initial feature points correspondence result based on the SC method, (i) initial feature points correspondence based on the LNS-RPM method, (j) feature points of the floating image generated by the moment based method, and (k) feature points of the reference image generated by the moment based method.

iteration, after updating these two vectors, the particle calculates its new velocity and position according to the following formulae:

$$\vec{v}_{k+1} = \varphi_0 r \vec{v}_k + \varphi_1 r (\vec{pbest}_k - \vec{x}_k) + \varphi_2 r (\vec{gbest}_k - \vec{x}_k),$$

$$\vec{x}_{k+1} = \vec{x}_k + \vec{v}_{k+1},$$

where k is the iteration number; φ_0 , φ_1 , and φ_2 represent the cognitive coefficients; r is a random value in interval $[0,1]$ according to uniform distribution; \vec{v} is the particle velocity vector; and \vec{x} is the particle position vector.

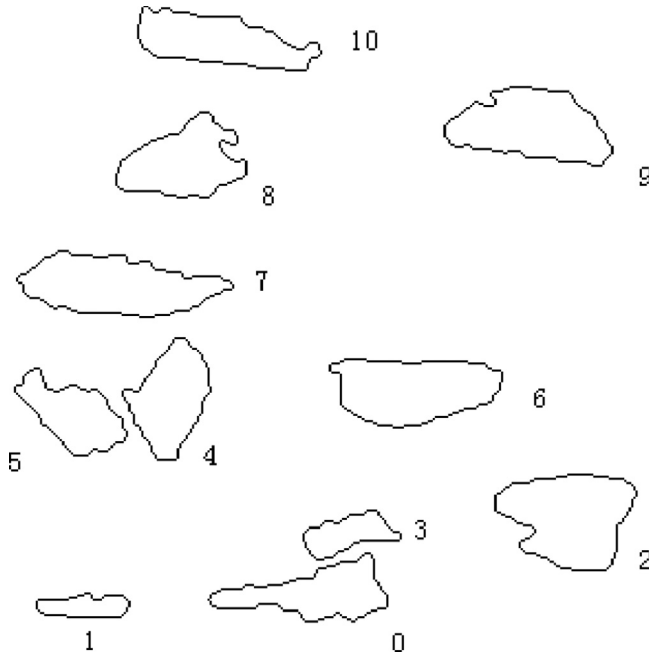


Fig. 9. The floating image of the composite.

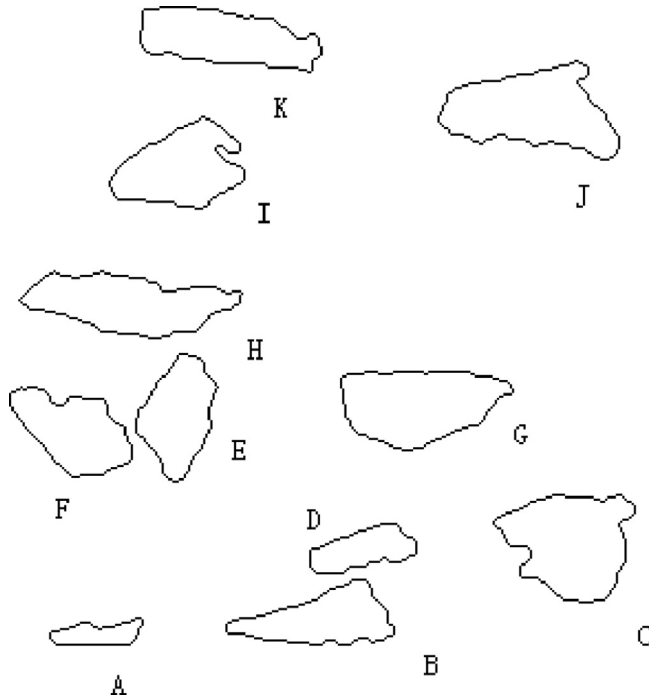


Fig. 10. The reference image of the composite.

3.2.2. Improved PSO algorithm

One problem observed in the standard PSO is that it can easily be trapped in local optima in certain optimization problems. The basic expression acquired by GEP usually contains several coefficients. Based on this fact, the concept of cooperation is applied to the standard PSO to create a family of CPSOs. The main concept of cooperation first views the solution of the problem as an n -dimensional vector, and the vector is subsequently split into its constituent components and assigned to multiple PSO populations. In this situation, the vector is split into its components such that the swarms optimize a 1-D vector of the solution vector [35]. Thus, all of the swarms must cooperate to compute the fitness of a particle because the contribution to the fitness in each dimension is not implicitly described. A valid solution vector can only be formed by the information gained from all swarms [36].

To accelerate the convergence of the CPSO algorithm, the opposition-based-learning (OBL) algorithm is adopted [37]. OBL is a technique that has been applied in several circumstances to enhance the performance of differential evolution. An improved version of the OBL-based CPSO (CPSOBL) is proposed such that in the half of the particles with the lowest fitness, the coefficient is replaced by its opposite (the anti-particle) in each iteration, as follows:

$$x' = a + b - x, \quad (7)$$

where $[a, b]$ is the value interval of the coefficient, and x is the coefficient of the lowest fitness.

Suppose the basic structure acquired by GEP usually has n coefficients; the solution vector is therefore an n -dimensional real number vector. Based on the concept of the CPSO and OBL, we introduce an improved PSO algorithm known as CPSOBL to complete the parameter optimization.

First, the n coefficients of the basic expression are optimized using the standard PSO algorithm; thus we acquire the initial n -dimensional solution vector. Second, the solution vector is split into n parts, each part is optimized by a swarm of m particles, and the remaining $n-1$ parts are fixed. We select the l best individuals of the population for every part, allowing for $l \times n$ combinations for construction of the composite n -dimensional vector. Third, OBL is used to increase the solution diversity. For each one-dimensional vector (i.e., a coefficient of

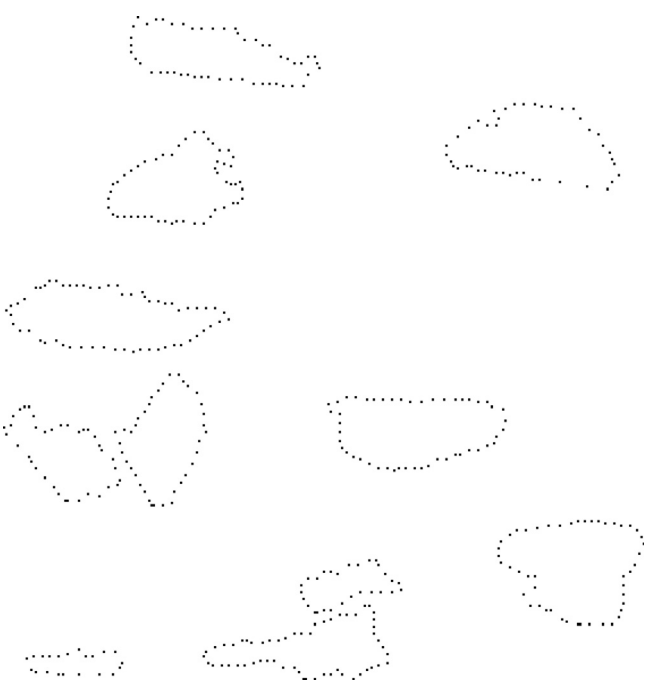


Fig. 11. The feature points of the floating composite image.

the basic expression), its opposition vector is calculated using Eq. (7). Thus, $2^k \times n$ combinations are available for constructing the composite n -dimensional vector. For the $2^k \times n$ -dimensional vector, we take the overlap rate as the fitness value. The final solution can be acquired based on the maximum fitness. If the maximum fitness is greater than the predefined threshold value, the final solution is taken as the initial

n -dimensional solution vector, and the algorithm is repeated until the termination criterion is satisfied.

By applying the cooperative method in the coefficient optimization of the basic expression, each particle in the CPSOBL contributes to the population not only as an entire item but also in each dimension. In addition, the opposition-based learning method increases the solution diversity of the entire algorithm. These methods ensure that the search space is searched more thoroughly and that the algorithm has an increased chance of finding the best result.

3.3. Formula discovery based on the hybrid evolutionary algorithm

In this study, the set of formulae can be obtained by a limited combination of the terminal set T and the function set F . Finding an optimal or near-optimal expression is accomplished using the GEP

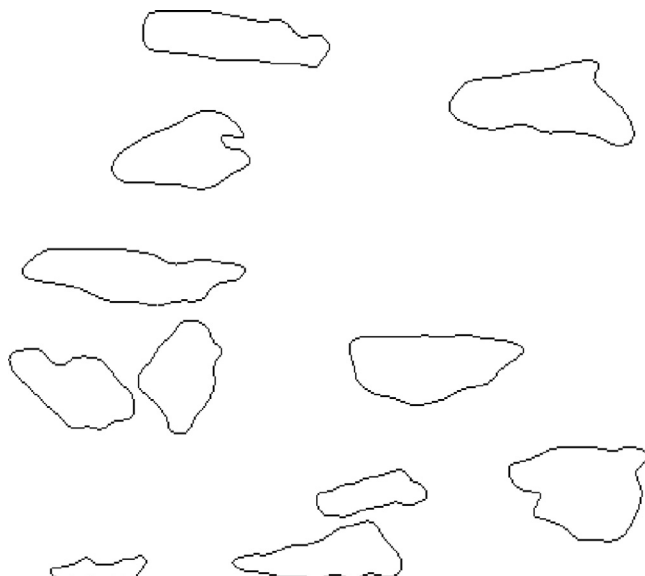


Fig. 12. The B-spline contours of the reference composite image.

Table 1
Correspondence of the contours in the reference and floating composite images.

The reference image	0	1	2	3	4	5	6	7	8	9	10
The floating image	B	A	C	D	E	F	G	H	I	J	K



Fig. 14. The feature points of the reference composite image.

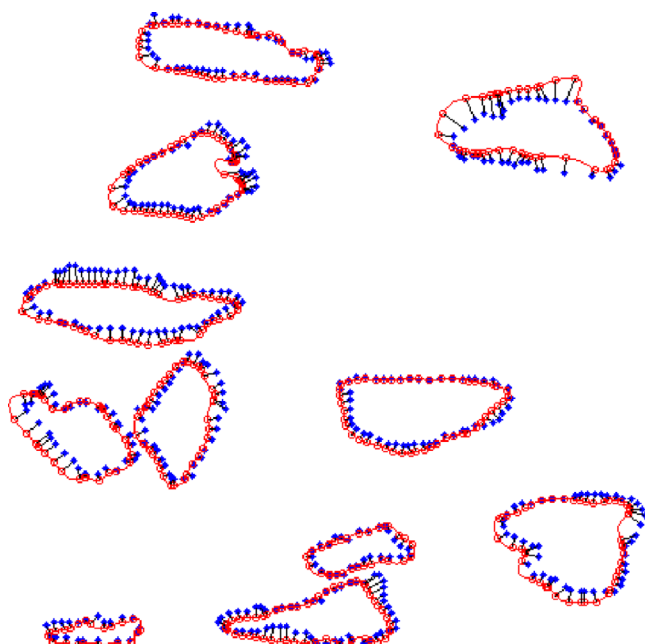


Fig. 13. The feature points detection on the B-spline contours of the reference composite image.

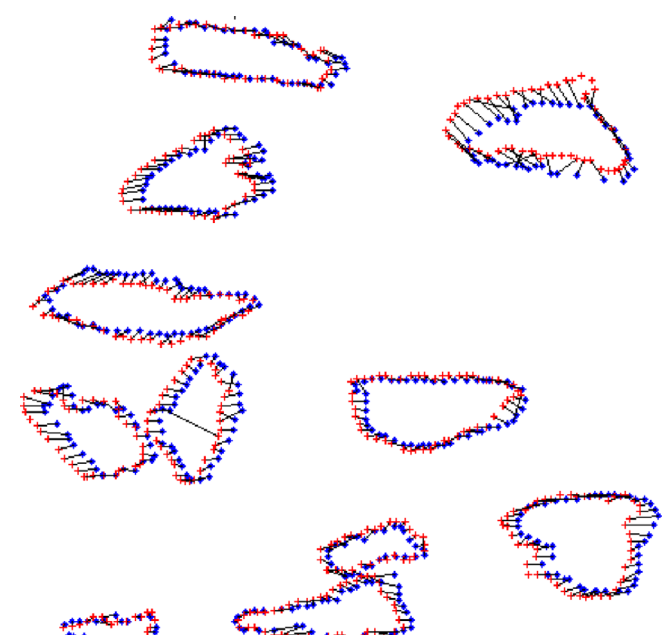


Fig. 15. The initial feature points correspondence result based on the SC method.

algorithm, and the parameters embedded in the structure are optimized using the CPSOBL algorithm. We refer to the overall algorithm as the CGEPSOBL. The search processes based CGEPSOBL are carried out as follows:

- Step 1. Create the program population PROG. Generate the initial population randomly according to the terminal set T and function set F ; each individual is a linear structure that includes

multiple logical expressions with different sizes to represent different logical rules.

- Step 2. Population evaluation. Every logical structure (in all individuals) is used to translate the floating point sets to the new location, and the fitness is calculated using Eq. (6). The fitness is based on the overlap rate between the polygon enclosed by the reference feature points and their corresponding polygon enclosed by the floating features (new location). The best program of the current population (that with the maximum fitness value) is denoted as PROGb. The best program found so far (elitist) is preserved in PeLROG.

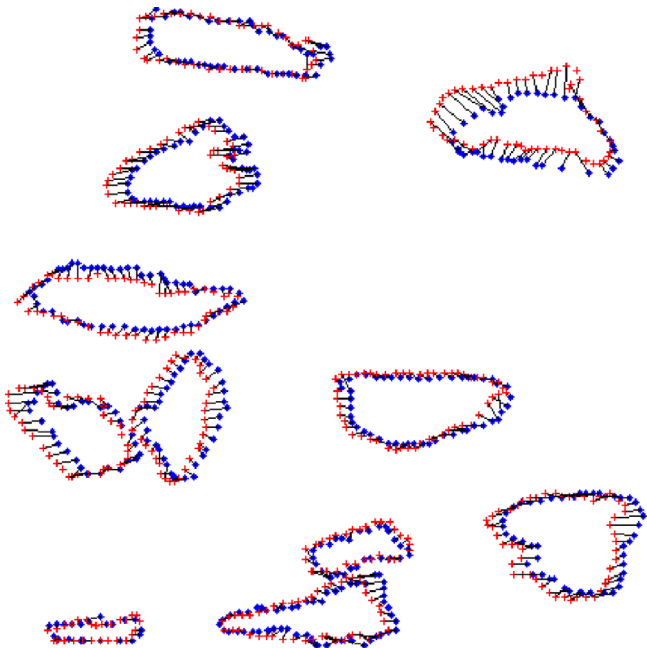


Fig. 16. The initial feature points correspondence based on the LNS-RPM method.

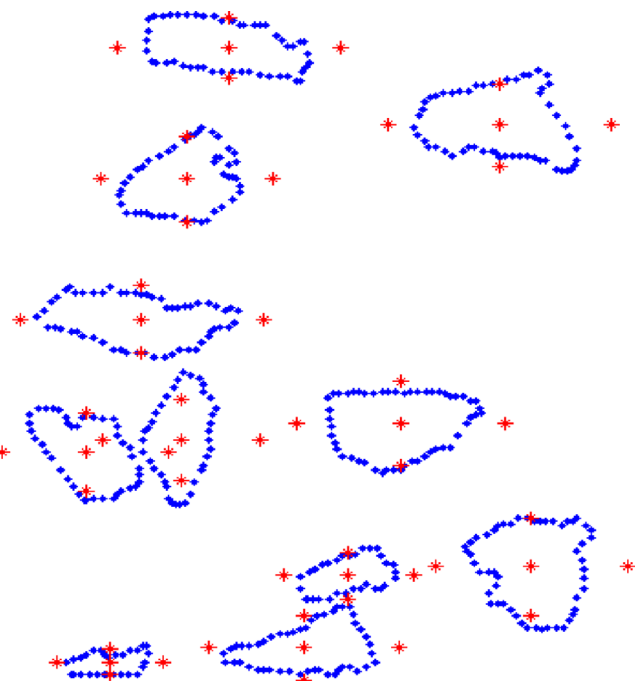


Fig. 18. The feature points of the reference image generated by the moment based method.

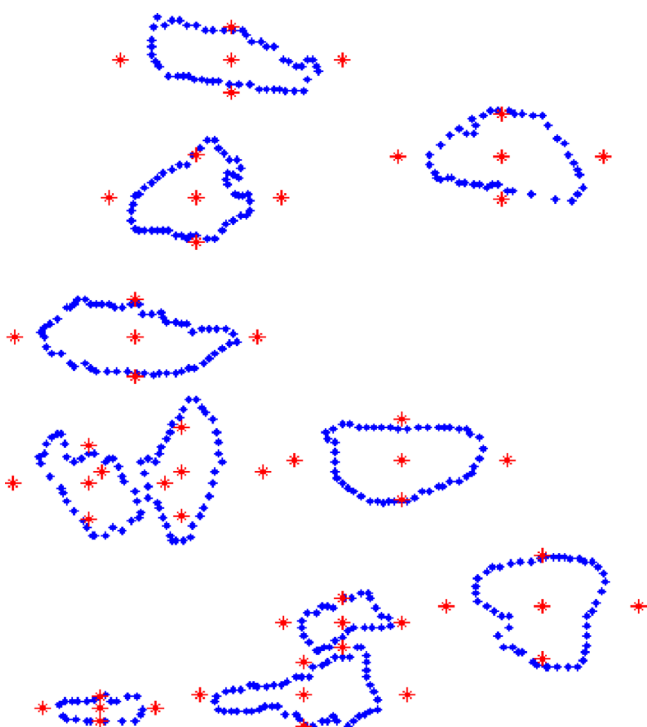


Fig. 17. The feature points of the floating image generated by the moment based method.

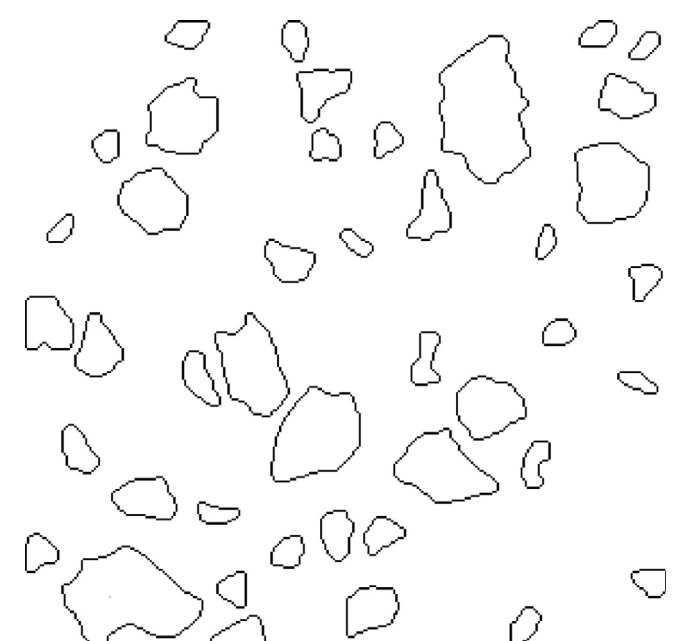


Fig. 19. The floating image of cement.

Step 3. Generate a set of candidate solutions randomly, select the d best individuals, and replace the same number of individuals in population PROG. The lower fitness individuals have higher probabilities of being replaced.

- Step 4. Genetic operations of crossover and mutation are performed between individuals to generate the better new population. The individuals denoted as PROGb and PeIROG have higher probabilities of being selected to participate.
- Step 5. Repeat the above procedure until a fixed number of program evaluations are completed, and the intermediate structure can be achieved.
- Step 6. The coefficients of the structure have an important impact on searching the optimal solution. Based on the initial n -dimensional solution vector acquired by the standard PSO algorithm, the CPSOBL algorithm is used to find the best solution of the coefficients of the basic optimized expression.

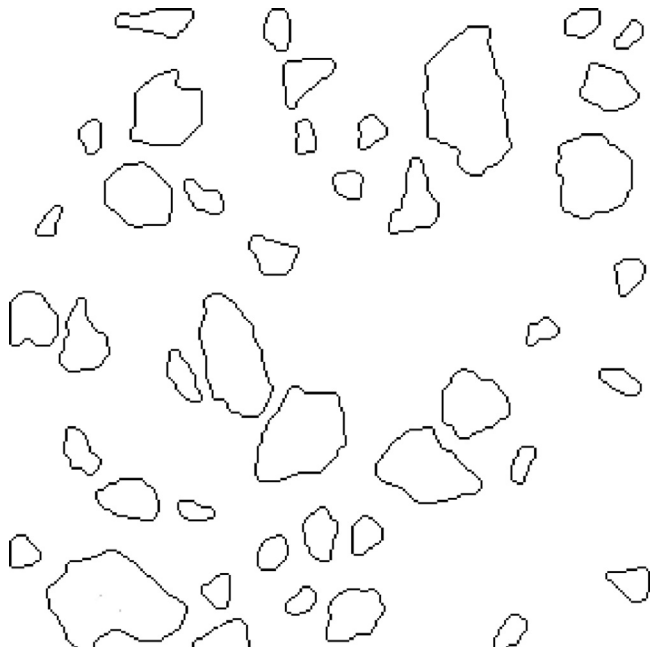


Fig. 20. The reference image of cement.

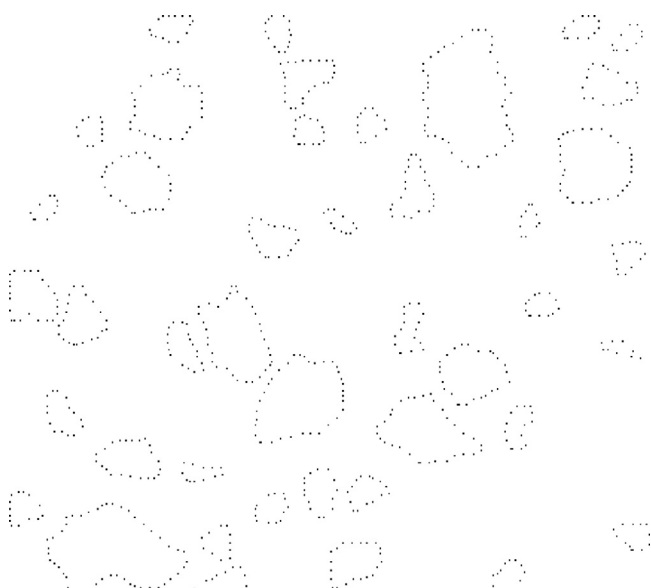


Fig. 21. The feature points of the floating cement image.

- Step 7. The floating point sets are translated using the final expression. Based on the new floating point set, a new generation is created, and the generation counter is increased. The process continues iteratively until a termination criterion is met. The termination criterion is that the fitness stagnate over 500 generations or the max generation is reached.

4. Experiments

In this section, a pair of hand contours, a pair of camel contours and two pairs of successive composite micrographs were studied.



Fig. 22. The B-spline contours of the reference cement image.

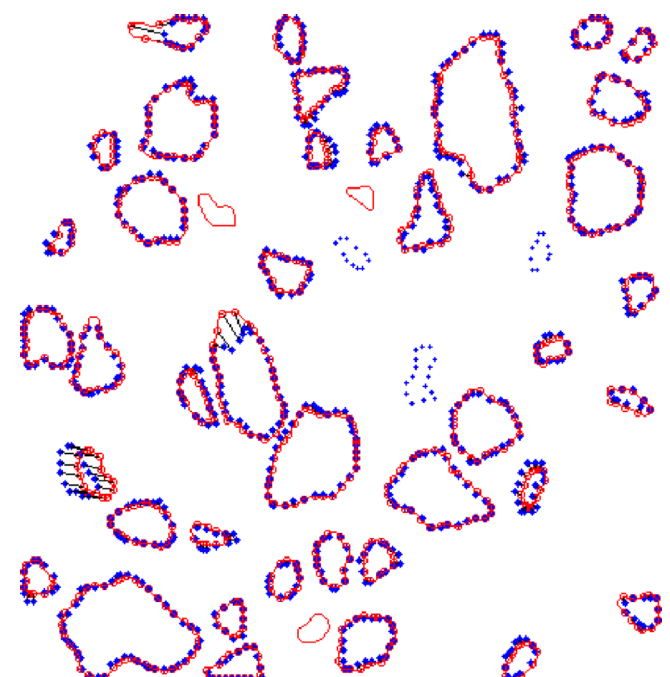


Fig. 23. The feature points detection on the B-spline contours of the reference cement image.

We provide the experimental results using the proposed algorithms for automated image registration. In the experiments, the floating images are shown in Fig. 8a, Fig. 9, Fig. 19 and Fig. 40a, and the reference images are shown in Fig. 8b, Fig. 10, Fig. 20 and Fig. 40b. In this paper, we use the overlap rate as the error measure. The overlap rate between two polygons can be computed based on the areas of the union and intersection of the polygons enclosed by the feature points. For comparison, the performance of our approach is compared with that of the Shape Context (SC) method [18], the LNS-RPM method [20] and the MEPCSP method [24].



Fig. 24. Feature points of the reference cement image.

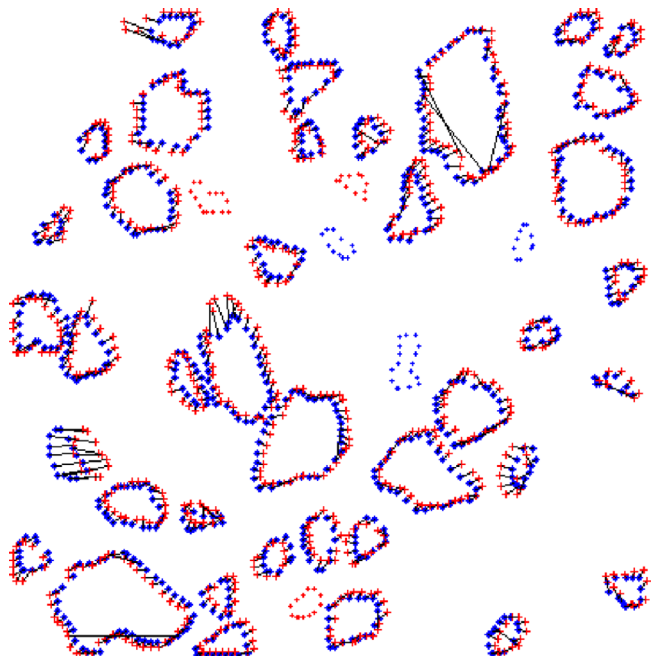


Fig. 25. The initial feature points correspondence based on the SC method.

4.1. Feature point sampling and assignment

The procedure presented in Section 2.2 was applied to the digital contours of the floating images and the reference images. The feature points of the images are all sampled by Eq. (2) in the experiment, the curvature threshold η is set to 0.26, the estimated curvature threshold ϵ is set to 2.0 and the maximum sample interval l is set to six. The contours in the reference images are also sampled using the curvature estimation algorithm, and a GMM-based continuous optimization algorithm [40] is used to approximate a planar B-spline curve for every reference contour. For every contour pair, the sampled feature points in the floating contour are mapped to the corresponding reference contour to find the foot points. Because the reference contours are described in a parameterized B-spline curve and the feature points in the

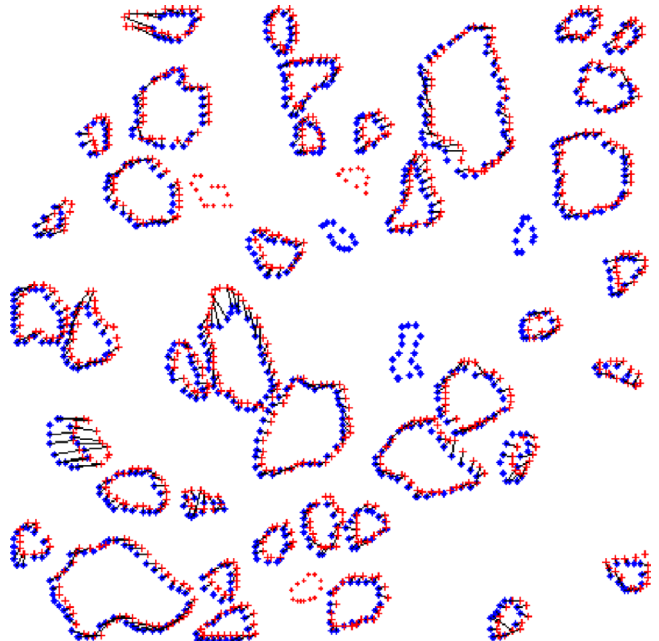


Fig. 26. The initial feature points correspondence based on the LNS-RPM method.

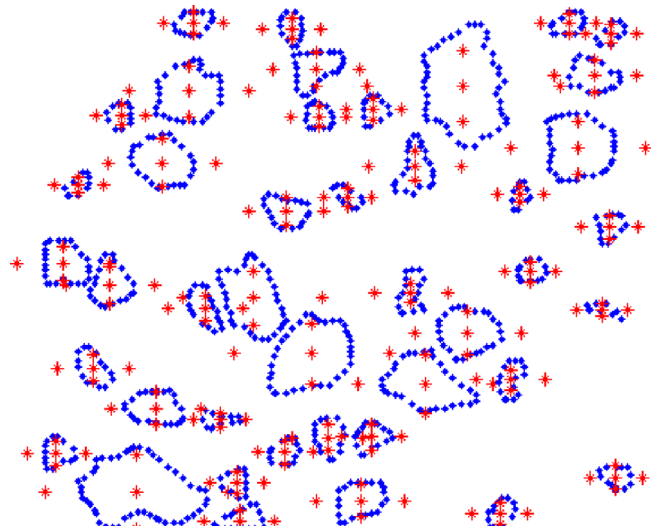


Fig. 27. The feature points of the reference image generated by the moment based method.

floating contours are sampled in series, the foot points can be detected in series.

Fig. 8 shows the feature point sampled and assignment of the hand data sets. **Fig. 8a** and b shows the floating and the reference images, respectively. **Fig. 8c** and d shows the feature points of the floating image acquired by Eq. (2) and the B-spline contour of the reference image. **Fig. 8e** shows the initial foot point of the floating feature points on the reference hand contour, and **Fig. 8f** highlights the marked part in **Fig. 8e** with magnified views. **Fig. 8g** shows the feature points of the reference image. **Fig. 8h** and i shows the initial matching result of the feature points based on the SC method and the LNS-RPM method, from which we can find some overt mismatch. **Fig. 8j** and k shows the feature points acquired by the moment-based technique [24], and those feature points will be used in the MEPCSP algorithm (similarly hereafter). The feature points in **Fig. 8j** and k are matched automatically because the feature points are the centroids of the contours and the axis endpoints of the contour ellipses [24].

Figs. 9 and 10 show a pair of composite images, and **Figs. 19 and 20** display a pair of cement images [42]. The feature points in

the floating image are shown in **Figs. 11 and 21**, and the B-spline contours of the reference images are shown in **Figs. 12 and 22**, respectively. For the multi-contour images, the contour correspondence algorithm described in **Section 2.1** was first used to find the matched contours. The correspondence of the contours in the composite floating image and reference image is shown in **Table 1**.

The correspondence of the feature points between the floating and the reference contours of the composite image and the cement image are shown in **Figs. 13 and 23**. The feature points of the reference image used for the SC method and the LNS-RPM method are shown in **Figs. 14 and 24**, respectively. **Figs. 15 and 25** show the initial correspondence results of the feature points based on the SC method for the composite image and the cement image, respectively. The initial correspondence results of the LNS-RPM method for the composite image and the cement image are shown in **Figs. 16 and 26**. **Figs. 17 and 18** show the feature points of the composite images acquired by the moment-based technique, and **Figs. 27 and 28** show the feature points of the cement images. The feature points in **Figs. 17, 18, 27 and 28** will be used in the MEPCSP algorithm. The correspondence information of contours and feature points are shown in **Table 2**.

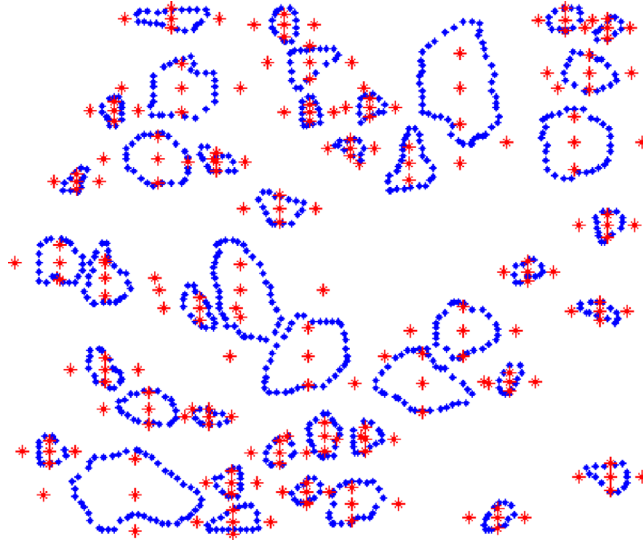


Fig. 28. The feature points of the reference image generated by the moment based method.

4.2. Contour registration based on the hybrid evolutionary algorithm

Given a number of feature point pairs from two images, the formulae of the registration model can be established using a two-stage evolutionary algorithm, the CGEPSOBL. In **Table 3**, we enumerate the main parameters of GEP in the hybrid algorithm. For the CPSOBL as the coefficient searching algorithm, the population size is set to 100, the maximum number of generations is set to 1000, φ_0 is set to 1, φ_1 is set to 1.8, and φ_2 is set to 1.6. The values of the parameters are all determined by experience and trial-and-error.

In this paper, the fitness is based on the overlap rate, described using Eq. (6). For comparison, the performance of our approach is compared with that of the SC method, the MEPCSP method and the LNS-RPM method. Based on the hand point sets shown in **Fig. 8e**, **Fig. 29a** and b shows the registration results of the handsets calculated by the CGEPSOBL, and **Fig. 29c** and d shows the registration result calculated by the SC, LNS-RPM methods, respectively. From the results, we observe that two methods of SC and LNS-RPM cannot acquire the correct results because of the initial mismatch of the feature points. **Fig. 29e** shows the

Table 2
Corresponding of contours and feature points.

	Number of contours in the floating image/number of contours in the reference image	Number of contour pairs	Number of feature points acquired by the algorithm described in Section 2.2		Number of feature point pairs for CGEPSOBL
			In the floating image	In the reference image	
The hand data sets	1/1	1	320	335	320
The composite data sets	11/11	11	432	489	432
The cement data sets	43/43	40	878	905	820

Table 3
Main parameters in GEP.

Function set	Terminal set	Length of chromosome	Iteration number	Population size	Crossover probability	Mutation probability	Linking function
$+, -, *, /, \text{square}, \text{sqrt}, \log, \cos, \sin$	x_0, x_1, a	84	10,000	200	0.30	0.20	$+, -, *, /$

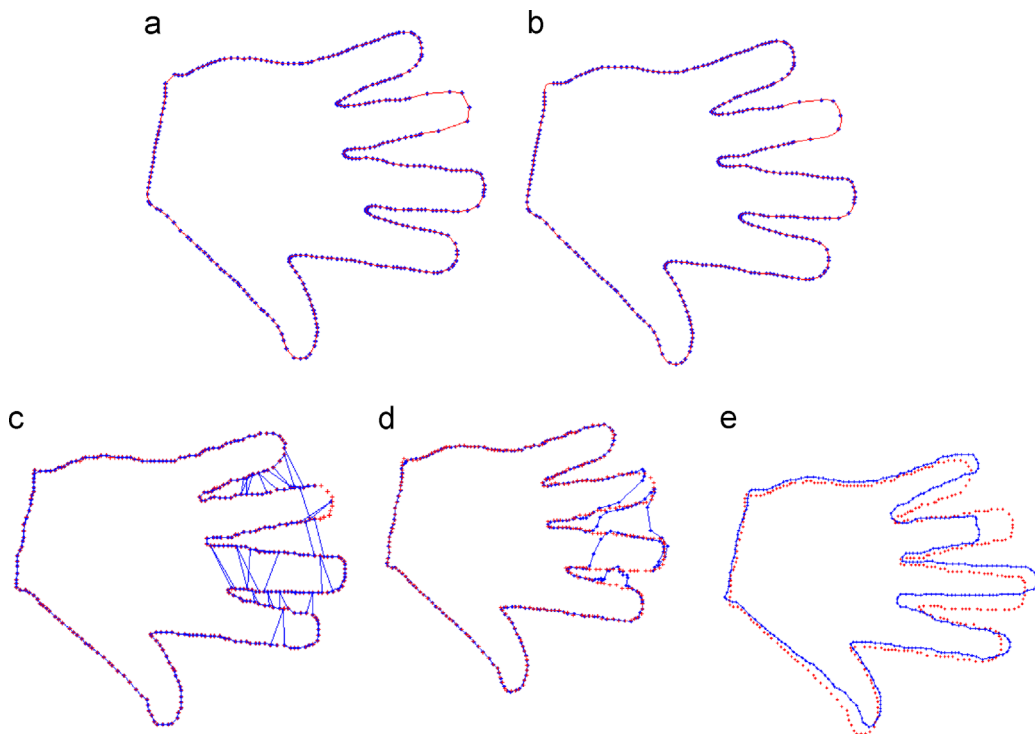


Fig. 29. Registration results of the hand data sets: (a) registration result by CGEPSOL in which the reference contour is described by feature points, (b) registration result by CGEPSOL with the reference contour described by a B-spline curve, (c) registration result by SC, (d) registration result by LNS-RPM, and (e) registration result by MEPCSP.

Table 4
The overlap error before and after registration.

Models	Overlap area	Method			
		CGEPSOBL	SC	LNS	MEPCSP
Hand	Before registration	4619.5	4612.8	4612.8	4612.8
	After registration	22.24	1884.1	3830.3	6056.7
Composite	Before registration	5804.9	5957.2	5957.2	5957.2
	After registration	37.35	635.22	1251.6	3086.3
Cement	Before registration	7387.6	7432.4	7432.4	7432.4
	After registration	45.26	736.31	2334.1	3203.3
Camel	Before registration	26,594	26,654	26,654	26,654
	After registration	384.12	10,108.6	19,344	9099.6

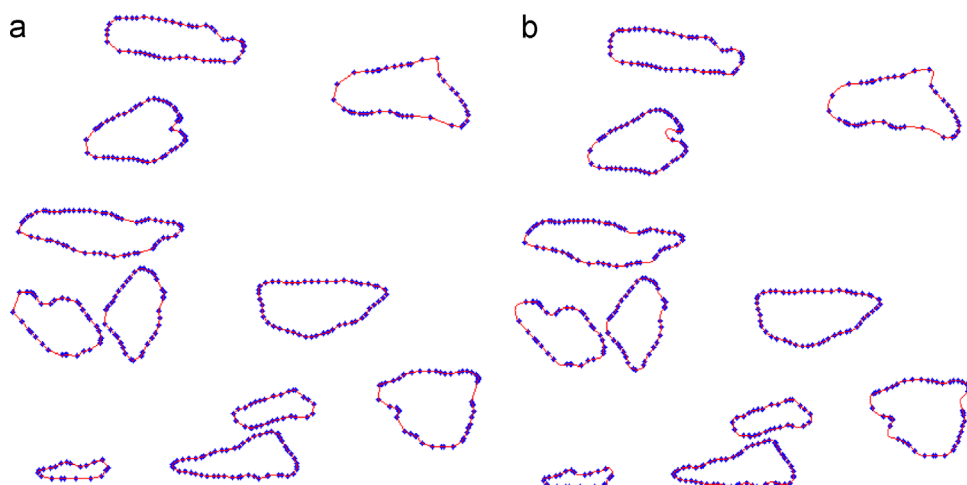


Fig. 30. Registration result of the composite image: (a) registration result by CGEPSOBL, (b) registration result by CGEPSOBL with the reference contour described by a B-spline curve.

registration result calculated by the MEPCSP algorithm from which we can find that this algorithm also cannot acquire an accurate result, the reason for this is that the number of the corresponding points is too small (for one contour, there are only five point pairs). Fig. 39 shows the overlap rate for our method and the comparison methods. To avoid execution dependence, 20 different runs of each CGEPSOBL were performed in every problem instance (and similarly hereafter). Table 4 shows the overlap error before and after registration. The overlap error is the nonoverlapping area of two corresponding contours.

Based on the point sets shown in Fig. 13, Fig. 30a and b shows the registration result of the composite image. Figs. 31–33 show the registration results calculated by the SC, LNS-RPM and MEPCSP

algorithms, respectively. From the figures, we observe a descending order of the registration results.

The third example is the successive cement image. The initial correspondence of the point sets for our method is shown in Fig. 23. Based on this information, Figs. 34 and 35 show the registration result calculated by the CGEPSOBL method. Based on correspondence shown in Figs. 25 and 26, the registration result calculated by the SC and the LNS-RPM methods are shown in Figs. 36 and 37. In addition, the registration result from the MEPCSP algorithm is shown in Fig. 38.

From the overlap rate described in Fig. 39, we arrive at the conclusion that the CGEPSOBL algorithm provides a competitive performance compared with that of the SC, MEPCSP and LNS-RPM methods. Moreover, because the high nonlinearity of the function set and their combinations in CGEPSOBL, the CGEPSOBL can produce a more accurate result.

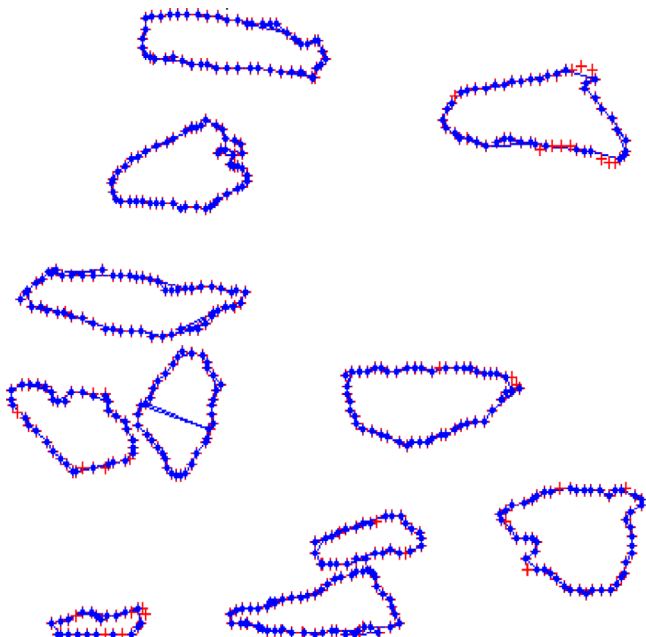


Fig. 31. Registration result by SC for the composite image.

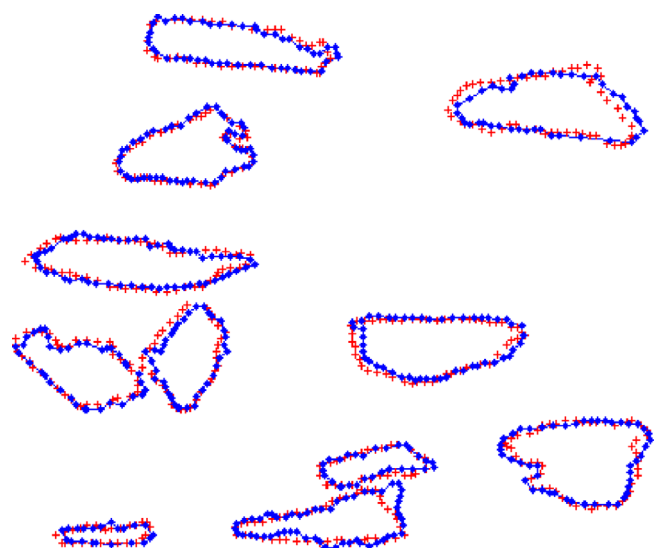


Fig. 33. Registration result by MEPCSP for the composite image.

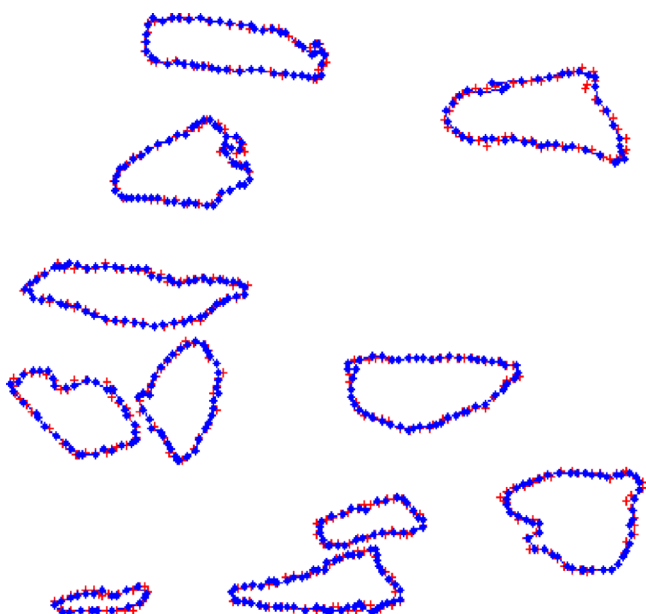


Fig. 32. Registration result by LMS-RPM for the composite image.

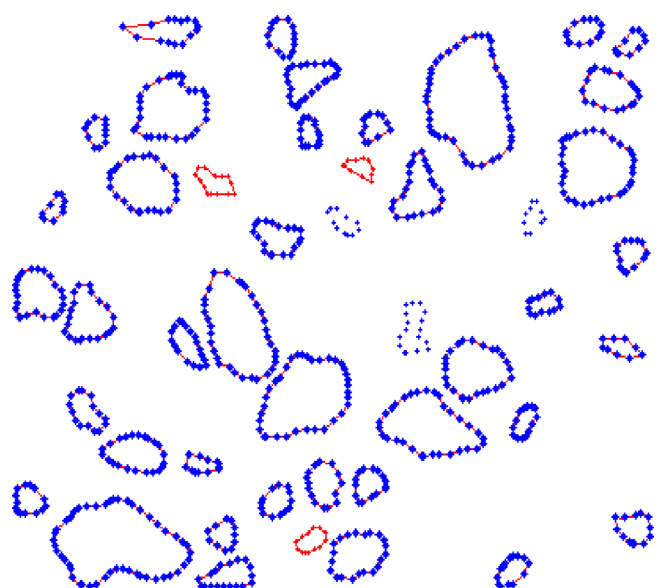


Fig. 34. Registration result by CGEPSOBL for the cement image.

4.3. Registration for complicated contours

To ensure the correct correspondence of the feature pairs from complicated contours (i.e., a feature pair that is located close together on one shape is mapped to points that are also closely located on the other shape), we segment the contours and calculate the feature pairs separately. As an example, Fig. 40a and b shows the feature points of the camel sets [43]. We acquire the segment points using the topology-preservation algorithm [41], and the results are shown in Fig. 40c and d. Based on the feature points and the segment points, we approximate the floating camel contour using the B-spline approximation algorithm with segment point interpolation, as shown in Fig. 40e. The correspondence between the segment points of the floating

contour and the reference contours is completed using the algorithm proposed in reference [39], and the result is shown in Fig. 40f. The feature points detection on the B-spline contour and the correspondence between the feature points are completed using the algorithm described in Section 2.2, and the result is shown in Fig. 40g. Fig. 40h shows the registration result of the camel calculated using the CGEPSOBL algorithm.

Fig. 41a shows the initial matching result of the feature points based on the SC method, and Fig. 41b shows the initial matching result of the LNS-RPM method; from both, we can observe the presence of mismatches. Fig. 41e and f shows the registration results from the SC and LNS-RPM algorithms, respectively. Fig. 41c and d shows the feature points of the floating and the reference camel contours generated by the method based on the moment



Fig. 35. Registration result by CGEPSOBL with the reference contours described by B-spline curves for the cement image.

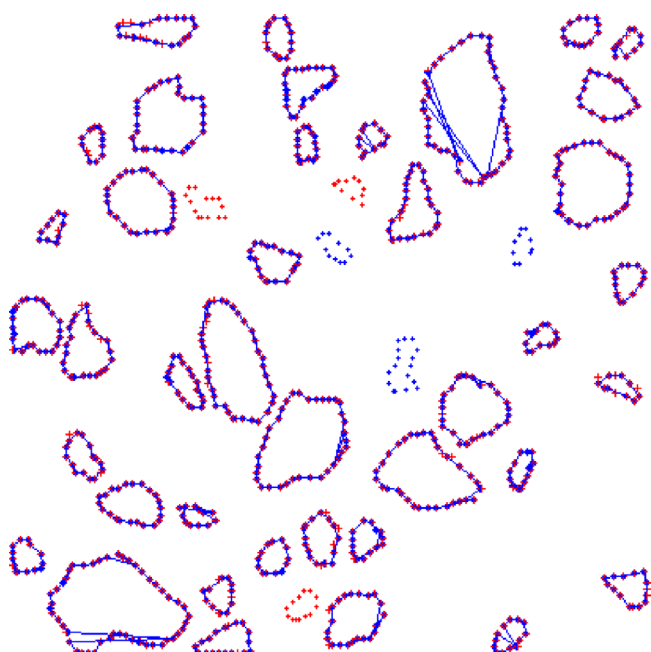


Fig. 36. Registration result by SC for the cement image.

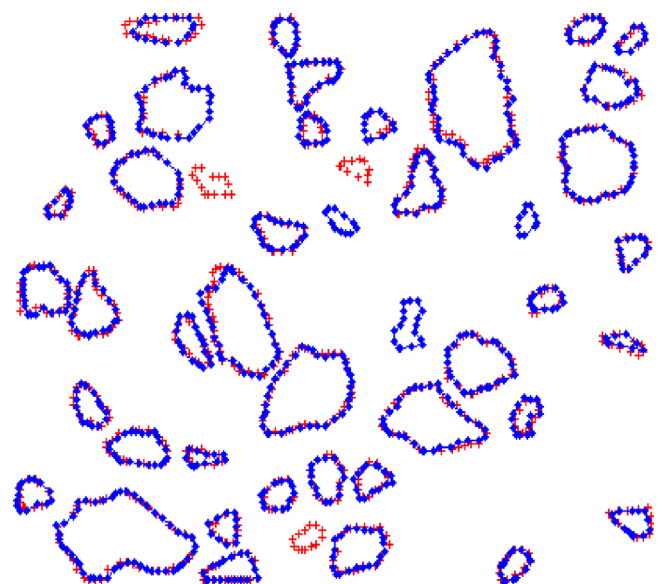


Fig. 37. Registration result by LMS-RPM for the cement image.

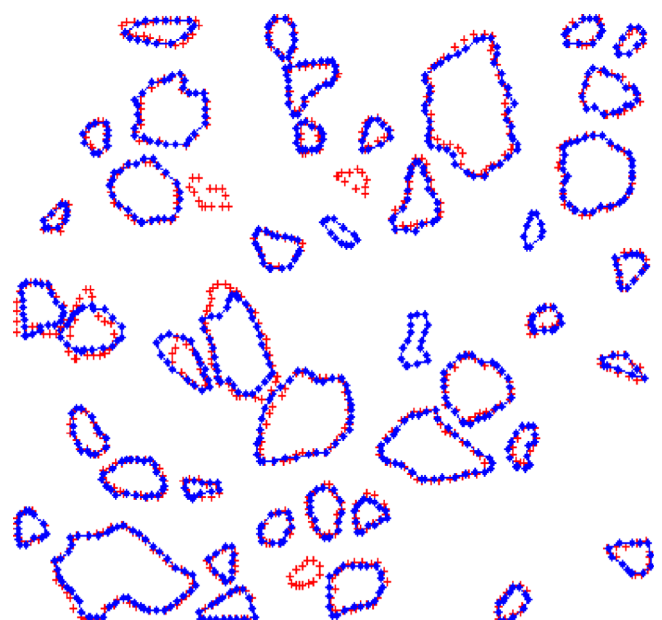


Fig. 38. Registration result by MEPCSP for the cement image.

technique. Based on the feature points of Fig. 41c and d, the registration result from the MEPCSP algorithm is shown in Fig. 41g.

In this paper, we consider the special case in which the shapes of interest are defined by one or multiple closed contours, the assignment of the corresponding points must preserve the cyclic ordering inherited from the contours. Because the methods of the SC, LNS-RPM and MEPCSP cannot preserve the cyclic order-

correspondence of feature points, we obtained bad results by using these methods. On the contrary, the algorithm of the foot-point-based feature point matching is an order-preserving method and the CGEPSOBL algorithm contains the powerful capability of formula discovery, we can obtain a correct and accurate registration result with these approaches.

5. Conclusions

This paper proposes a novel image registration pipeline based on a foot-point detection algorithm and a two-stage evolutionary algorithm. At the feature point detection stage, we propose a novel feature points extraction method based on the estimated curvature and the neighboring rule. The experimental results show that the method is able to obtain a representative and relatively even set of feature points to describe the entire contour. At the stage of determining pairs of feature points, we approximate the reference contours using B-spline curves, and an order-preserved foot-point detection method is subsequently used to extract the feature points corresponding to those of the floating contours. This method is an integrated algorithm that combines the feature point detection of the reference contours and the feature point correspondence of the reference contour and the floating contour. Because the reference contours are all described by B-spline curves and the floating feature points are also found in series, we can achieve an order-preserved correspondence. The experimental

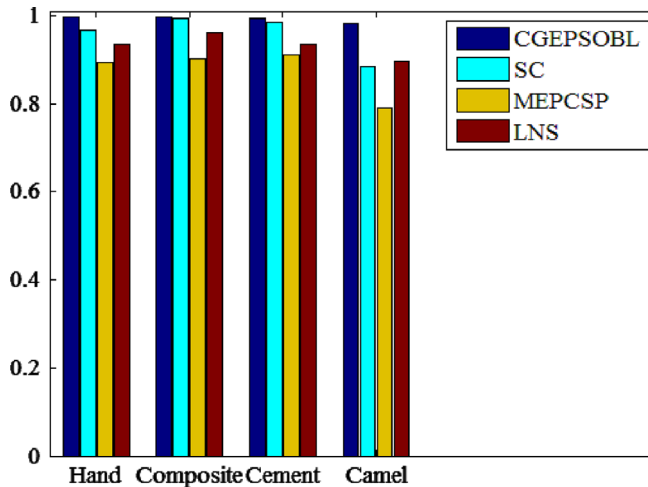


Fig. 39. The overlap rate.

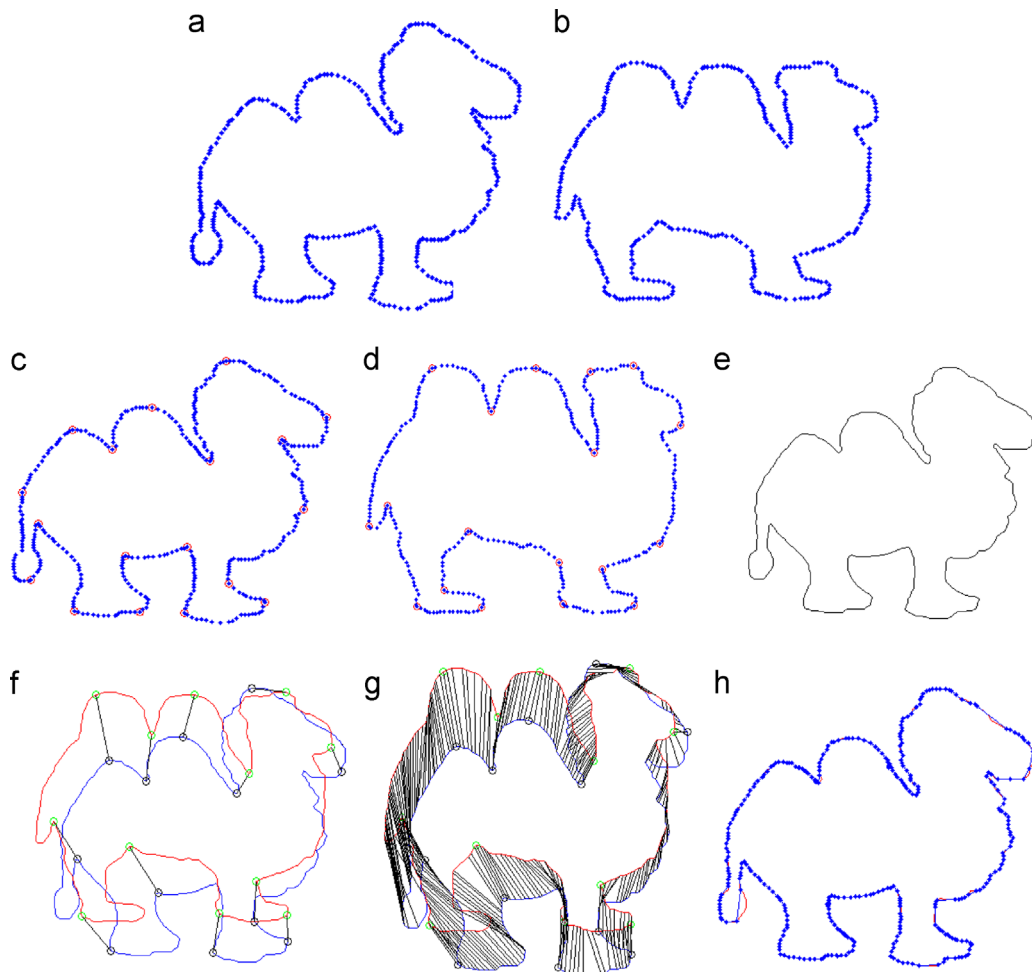


Fig. 40. Camel data sets: (a) feature points of the floating image, (b) feature points of the reference image, (c) segment points of the floating image, (d) segment points of the reference image, (e) B-spline contour of the floating image, (f) correspondence between the segment points, (g) feature points detection and correspondence on the B-spline contour, and (h) registration result by the CGEPSOBL method.

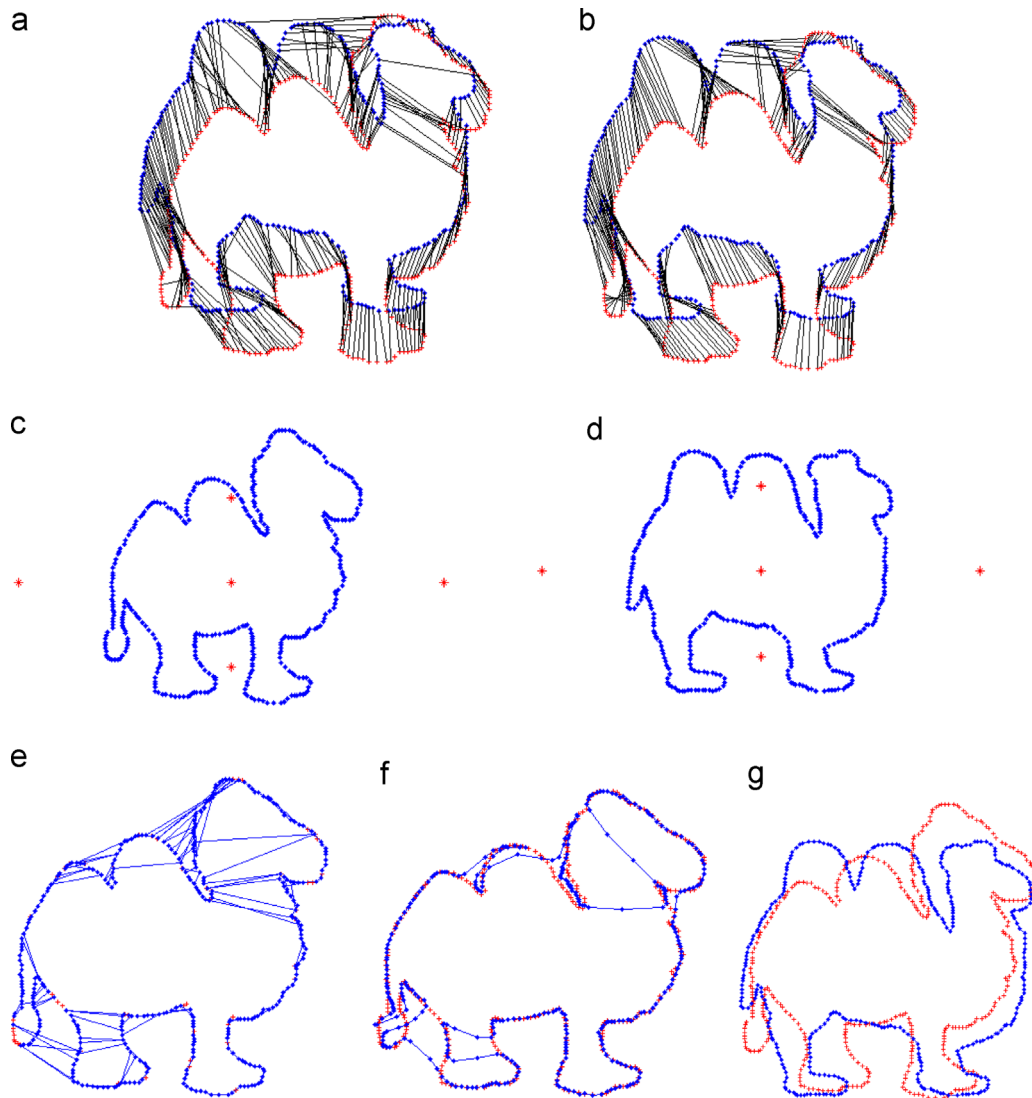


Fig. 41. Camel data sets: (a) initial feature points correspondence result based on the SC method, (b) initial feature points correspondence based on the LNS-RPM method, (c) feature points of the floating camel contour generated by the method based on the moment technique, (d) feature points of the reference camel contour generated by the method based on the moment technique, (e) registration result by the SC algorithm, (f) registration result by the LNS-RPM algorithm, and (g) registration result by the MEPCSP algorithm.

results also support this outcome. At the stage of finding the alignment transformation, we propose a two-stage evolutionary algorithm used to identify the registration formula for the reference image and the floating image. In the two-stage evolutionary algorithm, the basic structure is evolved using GEP, and the coefficients embedded in the expression are optimized by the CPSOBL. The algorithm has the ability to express a complicated formula structure that caters to the high nonlinearity of the non-rigid registration. The experimental results demonstrate that the developed registration pipeline produces competitive and highly accurate results compared with those of other non-rigid registration methods.

Acknowledgments

This research was supported by National Natural Science Foundation of China under contract (No. 61173078), Natural Science Foundation of Shandong Province under contract (Nos. ZR2010FM047 and ZR2011FL016).

References

- [1] S. Zokai, G. Wolberg, Image registration using log-polar mappings for recovery of large-scale similarity and projective transformations, *IEEE Trans. Image Process.* 14 (2005) 1422–1434.
- [2] W. Li, Z. Yin, Y. Huang, et al., Automatic registration for 3D shapes using hybrid dimensionality-reduction shape descriptions, *Pattern Recognit.* 44 (2011) 2926–2943.
- [3] Z.Q. Feng, B. Yang, Y.H. Chen, et al., Features extraction from hand images based on new detection operators, *Pattern Recognit.* 44 (2011) 1089–1105.
- [4] D.G. Lowe, Distinctive image features from scale-invariant key points, *Int. J. Comput. Vis.* 60 (2004) 91–110.
- [5] H.W. Kuhn, The Hungarian method for the assignment problem, *Nav. Res. Logist.* 2 (1955) 83–97.
- [6] G. Sanrom, R. Alquézar, F. Serratosa, A new graph matching method for point-set correspondence using the EM algorithm and Softassign, *Comput. Vis. Image Underst.* 116 (2012) 292–304.
- [7] H. Bay, A. Ess, T. Tuytelaars, L.V. Gool, Speeded-up robust features (SURF), *Comput. Vis. Image Underst.* 110 (2008) 346–359.
- [8] R. Horaud, F. Forbes, M. Igual, G. Dewaele, J. Zhang, Rigid and articulated point registration with expectation conditional maximization, *IEEE Trans. Pattern Anal. Mach. Intell.* 33 (3) (2001) 587–602.
- [9] C. Scott, R. Nowak, Robust contour matching via the order-preserving assignment problem, *IEEE Trans. Image Process.* 15 (2006) 1831–1838.
- [10] A. Fu, H. Yan, Effective classification of planar shapes based on curve segment properties, *Pattern Recognit. Lett.* 18 (1997) 55–61.

- [11] F.J.M. Cuevas, A.C. Poyato, R.M. Carnicer, R.M. Salinas, Contour simplification using a multi-scale local phase analysis, *Image Vis. Comput.* 26 (2008) 1499–1506.
- [12] W.Y. Wu, Dominant point detection using adaptive bending value, *Image Vis. Comput.* 21 (2003) 517–525.
- [13] W.Y. Wu, An adaptive method for detecting feature points, *Pattern Recognit.* 36 (2003) 2231–2237.
- [14] P.J. Besl, N.D. McKay, A method for registration of 3D shapes, *IEEE Trans. Pattern Anal. Mach. Intell.* 14 (1992) 239–256.
- [15] H. Chui, A. Rangarajan, A new point matching algorithm for nonrigid registration, *Comput. Vis. Image Underst.* 89 (2003) 114–141.
- [16] S.M. Li, C.L. Wang, K.C. Hui, Bending-invariant correspondence matching on 3-D human bodies for feature point extraction, *IEEE Trans. Autom. Sci. Eng.* 8 (2011) 805–814.
- [17] K. Delibasis, P.A. Avestas, G.K. Matsopoulos, Multimodal genetic algorithms-based algorithm for automatic point correspondence, *Pattern Recognit.* 43 (2010) 4011–4027.
- [18] S. Belongie, J. Malik, J. Puzicha, Shape matching and object recognition using shape contexts, *IEEE Trans. Pattern Anal. Mach. Intell.* 24 (2002) 509–522.
- [19] J. Xie, P.A. Heng, M. Shah, Shape matching and modeling using skeletal context, *Pattern Recognit.* 41 (2008) 1756–1767.
- [20] Y. Zheng, D. Doermann, Robust point matching for nonrigid shapes by preserving local neighborhood structures, *IEEE Trans. Pattern Anal. Mach. Intell.* 28 (2006) 643–649.
- [21] C. Ferreira, Gene expression programming: a new adaptive algorithm for solving problems, *Complex Syst.* 13 (2) (2001) 87–129.
- [22] G.H. Liu, Y.S. Wong, Y.F. Zhang, H.T. Loh, Adaptive fairing of digitized data points with discrete curvature, *Comput.-Aided Des.* 34 (2002) 309–320.
- [23] W.S. Li, S.H. Xu, G. Zhao, L.P. Goh, Adaptive knot placement in B-spline curve approximation, *Comput.-Aided Des.* 37 (2005) 791–797.
- [24] X.Y. Zhao, C.M. Zhang, Caiming, Y. Wang, B. Yang, A hybrid approach based on MEP and CSP for contour registration, *Appl. Soft Comput.* 11 (2011) 5391–5399.
- [25] C. Ferreira, Genetic representation and genetic neutrality in gene expression programming, *Adv. Complex Syst.* 5 (4) (2002) 389–408.
- [26] Yuehui Chen, Bo Yang, Ajith Abraham, Lizhi Peng, Evolutionary design of hierarchical TS fuzzy models using evolutionary algorithms, *IEEE Trans. Fuzzy Syst.* 15 (2007) 385–397.
- [27] Lizhi Peng, B.o. Yang, Lei Zhang, A. Yuehui Chen, Parallel evolving algorithm for flexible neural tree, *Parallel Comput.* 37 (5) (2011) 653–666.
- [28] H.F. Wang, E.R. Hancock, Correspondence matching using kernel principal components analysis and label consistency constraints, *Pattern Recognit.* 39 (2006) 1012–1025.
- [29] T. Huysmans, J. Sijbers, B. Verdonk, Automatic construction of correspondences for tubular surfaces, *IEEE Trans. Pattern Mach. Intell.* 32 (2010) 636–651.
- [30] V.E. Markaki, P.A. Avestas, G.K. Matsopoulos, Application of Kohonen network for automatic point correspondence in 2D medical images, *Comput. Biol. Med.* 39 (2009) 630–645.
- [31] H. Jia, P.T. Yap, D. Shen, Iterative multi-atlas-based multi-image segmentation with tree-based registration, *NeuroImage* 59 (2012) 422–430.
- [32] W.P. Wang, H. Pottmann, Y. Liu, Fitting B-spline curves to point clouds by curvature-based squared distance minimization, *ACM Trans. Graph.* 25 (2006) 214–238.
- [33] G.O. Mason, K.W. Wong, Image alignment by line triples, *Photogramm. Eng. Remote Sens.* 58 (1992) 1329–1334.
- [34] J. Kennedy, R. Eberhart, Particle swarm optimization, in: Proceedings of IEEE International Conference on Neural Networks, Piscataway, USA, 1995, pp. 1942–1948.
- [35] F. Bergh, A.P. Engelbrecht, A cooperative approach to particle swarm optimization, *IEEE Trans. Evolut. Comput.* 8 (2004) 225–239.
- [36] H. Gao, W. Xu, J. Sun, et al., Multilevel thresholding for image segmentation through an improved quantum-behaved particle swarm algorithm, *IEEE Trans. Instrum. Meas.* 59 (2010) 934–946.
- [37] H.R. Tizhoosh, Opposition-based learning: a new scheme for machine intelligence, in: Proceedings of the 2005 International Conference on Computational Intelligence for Modelling, Control and Automation, Vienna, 2005, pp. 695–701.
- [38] L. Todorovski, S. Dzeroski, Declarative bias in equation discovery, in: Proceedings of the Fourteenth International Conference on Machine Learning, San Francisco, USA, 1997, pp. 376–384.
- [39] A. Myronenko, X. Song, Point set registration: coherent point drift, *IEEE Trans. Pattern Mach. Intell.* 32 (2010) 2262–2275.
- [40] X.Y. Zhao, C.M. Zhang, B. Yang, P.P. Li, Adaptive knot placement using a GMM based continuous optimization algorithm in B-spline curve approximation, *Comput.-Aided Des.* 43 (2011) 598–604.
- [41] X. Bai, L.J. Latecki, W. Liu, Skeleton pruning by contour partitioning with discrete curve evolution, *IEEE Trans. Pattern Anal. Mach. Intell.* 29 (2007) 449–462.
- [42] D.P. BENTZ, S. MIZELL, S. SATTERFIELD, J. DEVANEY, W. GEORGE, P. KETCHAM, J. GRAHAM, J. PORTERFIELD, D. QUENARD, F. VALLEE, H. SALLEE, E. BOLLER, J. BARUCHEL, The visible cement data set, *J. Res. Natl. Inst. Stand. Technol.* 107 (2) (2002) 137–148.
- [43] L.J. Latecki, R. Lakamper, U. Eckhardt, Shape descriptors for nonrigid shapes with a single closed contour, in: Proceedings of IEEE Conference on Computer Vision Pattern Recognition, 2000, pp. 424–429.



Zhao Xiuyang is an associate professor of the Provincial Key Laboratory for Network-based Intelligent Computing. He received his B.Sc. degree in material science and engineering from the Shandong University of Technology of China in 1998, and Master and Ph.D. degrees in computational material science from the Shandong University of China in 2001 and 2006. His main research interests include computer graphic, machine learning, and skeletal tissue engineering.



Yang Bo is a professor and vice-president of University of Jinan, Jinan, China. He is the Director of the Provincial Key Laboratory for Network-based Intelligent Computing and also acts as the Associate Director of Shandong Computer Federation, and Member of the Technical Committee of Intelligent Control of Chinese Association of Automation. His main research interests include computer networks, artificial intelligence, machine learning, knowledge discovery, and data mining.



Shuming Gao is a professor of the State Key Laboratory of CAD&CC and the School of Computer Science and Engineering, Zhejiang University which is located in Hangzhou, China. He received his Ph.D. degree from the Applied Mathematics Department of Zhejiang University in 1990, and was a visiting professor in the Design Automation Lab of Arizona State University and IPK, Germany respectively in 2001 and 2006. Currently he is serving as an associate editor of ASME Transaction of JCISE. He is also the committee member of a number of international conferences including ACM SPM, IEEE SMI, PLM, CSCWD, CAD/Graphics, etc.



Yuehui Chen received his B.Sc. degree from the Department of mathematics, Shandong University in 1985, and Master and Ph.D. degrees from the School of Electrical Engineering and Computer Science, Kumamoto University of Japan in 1999 and 2001. During 2001–2003, he had worked as the Senior Researcher at the Memory-Tech Corporation, Tokyo. Since 2003 he has been a member at the Faculty of School of Information Science and Engineering, Jinan University, where he currently heads the Computational Intelligence Laboratory. His research interests include Evolutionary Computation, Neural Networks, Fuzzy Logic Systems, Hybrid Computational Intelligence.